Pioneering Geothermal Energy Potential Study in Sudr Oil Field, Sinai, Egypt

Ahmed Shawky[1,2], César R. Chamorro[1], Francisco Javier Rey-Martinez[1], Mohamed Darwish[2], Mohamed Abdel Zaher[3], Mohamed Al Deep[3], Tamer Nassar[2]

[1] Department of Energy Engineering and Fluid Mechanics, School of Industrial Engineering (EII), University of Valladolid (UVa), Valladolid, Spain.

[2] Geology Department, Faculty of Science, Cairo University, Giza, Egypt.

[3] National Research Institute of Astronomy and Geophysics (NRIAG), Helwan, Cairo, Egypt

ahmedshawky.mohamed@uva.es

Keywords: *Gulf of Suez Rift, Sinai, Sudr Oil Field, 3D Structural Model, Geothermal Gradient, Resistivity Logs, Abandoned Oil Wells, Geothermal Power Potential*

ABSTRACT

Sudr oil field hosts one of Egypt's most significant geothermal features: Sudr-22 well (Ras Sudr sulfur water), originally drilled for oil and now producing 86 °C hot water. Located along the Gulf of Suez Rift, the area benefits from a high geothermal gradient due to its position on a structural high at the footwall of a major rift-related fault (AMSF) and its proximity to a significant hotspot just west of the field.

This study presents a comprehensive 3D geological model of the field, developed through seismic interpretation and well log data analysis. The model delineates the structural architecture, elaborating three northwest-trending rift-parallel faults that encompass a significant horst and secondary intra-horst structures. These structures facilitated the formation of localized geothermal compartments, where thermal water rises from wells accessing different geothermal reservoirs. Temperature data and gradient analysis reveal a geothermal gradient of 50 °C/km, indicating the potential to access a 70-80 °C reservoir within the Eocene reservoir at a depth of approximately 1 km. Higher temperatures of more than 120 °C may be reached by penetrating the deeper Nubian reservoir, located at a depth of approximately 2 km.

Additionally, resistivity analysis using well logs reveals distinct trends in the studied wells related to the geothermal environment. Notably, resistivity increases in front of the Eocene geothermal reservoir and evaporite zones in the Miocene strata, while cap rocks primarily composed of shaly and marly materials exhibit lower resistivities. This information was crucial for predicting additional geothermal reservoirs within the field.

The geothermal potential assessment estimates a recoverable thermal energy of approximately 6.3 PJ (6.7 MW) for the P50 scenario, with P10 and P90 estimates of 2.9 PJ (3 MW) and 12.1 PJ (12.8 MW), respectively, over a 30-year project lifespan. This power plant would be very beneficial to supply clean power to nearby households and touristic resorts. Sudr field thus emerges as one of Egypt's most promising sites for geothermal development. The opportunity to repurpose abandoned oil wells -especially those already producing thermal water- could significantly lower development costs. Additionally, the site offers a unique case study for geothermal–oil co-production, emphasizing the potential of oil fields to support sustainable energy initiatives.

1. INTRODUCTION

With an estimated 20-30 million abandoned oil and gas wells globally representing significant decommissioning liabilities and untapped geothermal potential, the strategic repurposing of existing oil field infrastructure offers a scalable solution to simultaneously address environmental responsibilities, reduce drilling costs, and advance energy transition goals. While geothermal energy demand continues to grow, the strategic reuse of oil field assets represents both an economic imperative and an environmental opportunity of international importance (Santos et al., 2022; Aydin et al., 2024; Meenakshisundaram et al., 2024; Boutot and Kang, 2025)

Sudr oil field is one of three important and adjacent development leases areas located in Sinai Peninsula, Egypt named Sudr, Matarma and Asl (Fig. 1). It was discovered in 1945 based on based on positive gravity anomaly (El Ayouty, 1990). It is owned by the Egyptian general petroleum company (GPC). The field occupies an important geosetting at the eastern rift margin of the Gulf of Suez rift, on the footwall of a major rift-related fault which we denoted as Ayun Musa-Sudr Fault (AMSF) (Fig. 2).

Figure 1: Location map of Sudr Oil Field situated along the eastern shore of the Gulf of Suez Rift, with the positions of the wells analyzed in this study. Field photos are attached showing Sudr-22 well, the main geothermal manifestation in the field (86 °C) and one of the geothermal lakes around.

The field is geologically a part of the so called Sudr rift block which is one of the rift blocks of the Gulf of Suez rift. The Sudr block have consistent SW dip direction and belong to

the northern (SW tilted) half graben of the Suez Rift. Almost all the exposed rocks in this block are Miocene in age (both Miocene clastics and Miocene evaporites) and have consistent SW dip. The Miocene evaporites have gentler dip compared to the Miocene clastics (2-4° and 4-12° respectively). The coastal area close to the Gulf of Suez shore is largely covered with Quaternary deposits (Fig. 2) (Moustafa, 2004). The stratigraphic section features both clastic and carbonate formations ranging in age from recent to Paleozoic. The oil entrapments are mainly in three reservoirs, which are the Eocene reservoir composed of fractured limestone, the Lower Miocene Nukhul Fm. composed of sandstone and conglomerate, and the Lower Miocene Asl Fm. Composed of sandstone and limestone (EGPC, 1996). On the other side, the formations which are regarded as the water aquifers in the field are the Nubian Sandstone of Paleozoic to Early Cretaceous in age, the Eocene reservoir, some horizons of both Upper Cretaceous and Miocene ages (Issar et al, 1971, ElZarka, 1975, El-Kiki et al., 1992), these reservoirs showed considerable thicknesses and water saturation in many wells of Sudr field (EGPC, 1996).

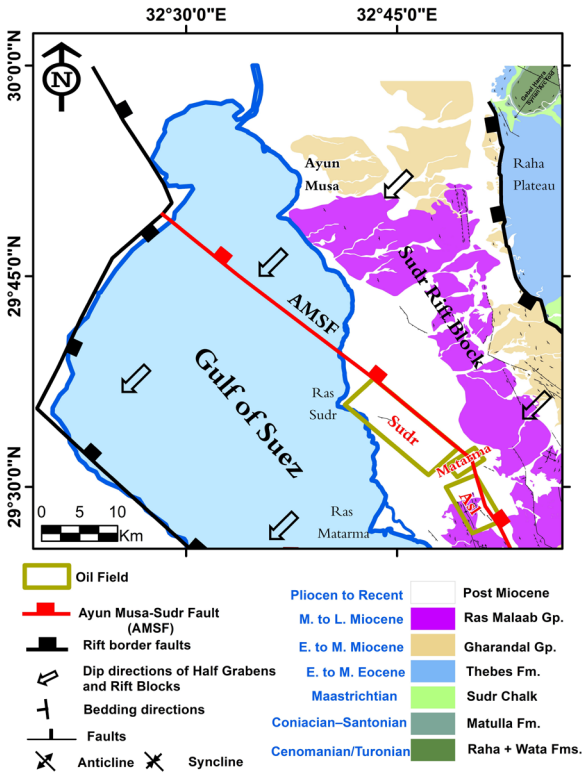

Figure 2: Geologic map of Sudr Oil Field and its vicinities showing the exposed rock unit and different structural elements, adapted from Moustafa (2004).

Resistivity wireline logging plays a crucial role in geothermal energy exploration and development by characterizing subsurface electrical properties that are essential for identifying and evaluating geothermal resources. This technique measures the electrical resistivity of rock formations and fluids in boreholes, providing valuable insights into reservoir characteristics. Geothermal activity alters the resistivity of rock formations due to the presence of different minerals formed under varying temperature conditions.

Three-dimensional structural modeling is essential for geothermal energy exploration as it provides critical insights into subsurface reservoir architecture and fluid flow pathways. By simulating the geometry of faults, fractures, and rock layers, 3D structural models enable accurate predictions of heat flow and fluid dynamics in geothermal systems, reducing exploration risks and costs. 3D modeling tools enable dynamic representation of geothermal resource understanding throughout a project's lifecycle, continuously integrating new data from surface exploration, drilling, and laboratory analyses to refine resource characteristics and validate previous assumptions. The evolving 3D model serves as the foundation for all strategic decisions, from well placement and geophysical survey planning to reservoir simulation optimization, ensuring that each phase of geothermal development is based on the most current and comprehensive understanding of the subsurface resource. (e.g. Jolie et al, 2012; Moeck, 2014, Poux and O'brien, 2020; Poux and Banks, 2022).

Sudr field comprises more than forty wells, three of which produced thermal waters and therefore were abandoned, these are Sudr 9, Sudr 15, Sudr 22 (Fig. 1). The measured temperature by the authors at the well head of Sudr-22 well was 86 °C.

This paper aims to understand the structural architecture of Sudr oil field in Sinai Peninsula through 3D structural modeling and to analyze the resistivity signatures of geothermal reservoirs using resistivity logs of thermal wells in the field. Moreover, it provides an assessment of the geothermal energy potential of the Sudr oil field for future geothermal development.

2. METHODOLOGY

The study relied on raw seismic and well logs for Sudr oil field provided by Egyptian General Petroleum Corporation (EGPC) and the Egyptian General Petroleum Company (GPC). Thirty 2D seismic lines were interpreted using Schlumberger Petrel software (Academic License no: 3-3797384; provided to the Geoinformatics lab of the Geology Department at Cairo University) to delineate the structural configuration of Sudr oil field. Key reflectors corresponding to the tops of the key horizons; the Eocene and Nubian Sandstone formations were identified and mapped, incorporating fault interpretations supported by formation tops from the well logs. These structural interpretations were subsequently converted into 2D structural depth maps, which were used to construct a 3D geological model. This model facilitated a comprehensive visualization of the subsurface geometry and fault architecture, enhancing the understanding of the structural framework and its implications for geothermal fluid flow inside the field.

The temperature calculations were based on a linear geothermal gradient model, utilizing the geothermal gradient of 50°C/km reported by Boulos (1990) for Sudr field, with a mean surface temperature of 26°C where the temperature at any given depth follows the relationship:

$$T = MST + (Z \cdot GG)$$

Where T is the temperature at a given depth (Z) in km, MST is the mean surface temperature in °C and GG is the geothermal gradient (°C/km).

Analysis of resistivity well logs of four abandoned oil wells (Sudr 9, Sudr 15, Sudr 22, and West Sudr-1) using Petrel software played a major role in geothermal reservoir characterization. These logs are of both shallow and deep resistivity logging. Resistivity variations were correlated with geothermal signatures to identify thermal water zones and predict additional reservoirs. Cap rocks were identified based on resistivity signatures. Moreover, lithology visualization of each stratigraphic zone interpreted from the composite logs of the wells supported the resistivity analysis and enhanced the overall petrophysical interpretation.

The 3D structural model was integrated with temperature data calculated as a function of depth using the estimated geothermal gradient. The depth values from the 3D reservoir models were combined with the derived geothermal gradient to compute formation temperatures at each grid point, subsequently generating comprehensive temperature distribution maps for both reservoir horizons. This approach enabled the spatial visualization of thermal variations across the geothermal reservoirs and facilitated the identification of optimal zones for potential geothermal energy extraction within the oil field.

Finally, Monte Carlo simulation was carried out to estimate geothermal potential by sampling from probability distributions of key reservoir parameters. The calculation considered both rock and fluid thermal energy content, applied a recovery factor of 0.12, and assumed a 30-year project life. Results are presented as probabilistic estimates (P10, P50, P90) to support risk-based decision making for geothermal development in Sudr oil field.

The total recoverable thermal energy was calculated by combining the heat stored in the rock matrix (E_{rock}) and pore fluids (E_{fluid}), The total heat in place (E_{total}) was estimated as:

$$E_{total} = E_{rock} + E_{fluid}$$

Where the rock matrix thermal energy is calculated using:

$$E_{rock} = \rho_{rock} \times C_{p\,rock} \times V_{rock} \times (T_{res} - T_{inj})$$

And the pore fluid thermal energy contribution is:

$$E_{fluid} = \rho_{fluid} \times C_{p\,fluid} \times V_{fluid} \times (T_{res} - T_{inj})$$

Where: ρ_{rock} and ρ_{fluid} are rock and fluid densities, $C_{p\,rock}$ and $C_{p\,fluid}$ are specific heat capacity of rock and fluid, V_{rock} and V_{fluid} refer to the volumes occupied by the solid rock matrix and the pore fluid, within the total reservoir volume, respectively. T_{res} and T_{inj} are the reservoir temperature (°C) and Injection temperature (°C), respectively.

The effective reservoir volumes are determined by:

$$V_{rock} = A_{eff} \times h \times (1 - \varphi)$$

$$V_{fluid} = A_{eff} \times h \times \varphi$$

Where: A_{eff} is the effective reservoir area (m²), h is the reservoir thickness (m), and φ is the effective porosity (dimensionless).

A recovery factor (R_f), modeled as a probability distribution to reflect extraction uncertainties, was applied to account for the fraction of heat that can be feasibly produced ($E_{recoverable}$):

$$E_{recoverable} = E_{total} \times R_f \times \eta_{conv}$$

Where R_f represents the thermal recovery factor (accounting for heat extraction efficiency, reservoir connectivity, and operational constraints) and η_{conv} denotes the thermodynamic conversion efficiency for power generation systems.

The sustainable power output over the project lifetime (P_{avg}) is calculated as:

$$P_{avg} = E_{recoverable} / (t_{project} \times 365 \times 24 \times 3600)$$

Where $t_{project}$ represents the operational lifetime (30 years) and the denominator converts to seconds for unit consistency.

The probabilistic assessment employed 10,000 Monte Carlo realizations to capture parameter uncertainties. Key uncertain variables were modeled using triangular probability distributions based on geological interpretation and reservoir characterization data. The effective reservoir area was calculated to reflect the fault-bounded reservoir geometry in the area covered by the three thermal wells. Average porosity of 25 for the Eocene reservoir in Sudr field (El Ayouty, 1990) was used. Eocene reservoir thickness in the range 100-300 m (EGPC, 1996) was used. The maximum geothermal gradient 50°C/km (Boulos, 1990); mentioned previously, was considered. The recovery factor (R_f) was estimated to be in the range of 8-20% (mode: 12%) representing extraction technology limitations and reservoir physics. The rock density (ρ_{rock}) of limestone of the Eocene reservoir was estimated to be 2650 kg/m³ while the rock specific heat capacity ($C_{p\ rock}$) was estimated as1000 J/kg·°C. The conversion efficiency (η_{conv}) was taken as 10-15% (mode: 12.5%; Zarrouk and Moon; 2014) assuming a binary cycle geothermal system. Table 1 lists all the parameters used in the simulation.

Parameter	Units	Minimum	Most Likely	Maximum
Reservoir Properties				
Effective Area	km²	0.5	2.0	8.0
Geothermal Gradient	°C/km	30	40	50
Porosity	%	8	18	25
Reservoir Thickness	m	100	200	300
Hot Water Zone Thickness	m	-	150	150
Temperature Parameters				
Surface Temperature	°C	26	26	26
Wellhead Temperature	°C	86	86	86
Heat Loss	°C	2.5	2.5	2.5
Reservoir Depth	km	1.0	1.0	1.0
Recovery Factor	-	0.08	0.12	0.20
Project Lifetime (fixed)	years	30	30	30

Table 1: Input Parameters for Monte Carlo Simulation for Sudr Oil Field Geothermal Assessment.

3. RESULTS AND DISCUSIION

3.1. Structural Model

The 3D structural model identifies three northwest-trending, rift-parallel faults traversing the area. These faults bound a prominent horst block and associated intra-horst secondary

structures (Fig. 3). The three faults are denoted as F-1, F-2 and F-3 from northeast to southwest.

F-1 faut constitutes a part of a large rift-related fault bounding Sudr oil field to the northeast. Numerous subsidiary faults associated with these major faults exhibit bifurcation or compensation patterns. The entire structure appears as a large southwest-dipping horst structure is bounded by two faults: the up-dip F-1 fault, which throws to the northeast, and the down-dip fault F-3, which throws to the southwest. The interplay of structural activity created a dramatic topography, where elevated blocks of crust (horsts) rise above the surroundings. Two horst structures host the three thermal wells (Sudr 9, Sudr 25, and Sudr 22), as depicted in Fig. 3. Horsts, as uplifted fault blocks, are characterized by extensive fracturing and faulting along their boundaries, providing enhanced permeability pathways that facilitate deep circulation of geothermal waters. These structural features allow water to penetrate to depths where it encounters elevated geothermal gradients, becoming heated through contact with deeper, warmer rock formations or proximity to heat sources at depth. However, it is worth mentioning that in sedimentary systems, geothermal gradients are typically lower than in volcanic areas. The fault systems associated with the horst structures not only enable deep water infiltration but also create natural conduits for heated fluids to ascend back toward the surface. Additionally, the structural complexity of horst blocks often coincides with areas of increased crustal thinning or elevated heat flow, further contributing to the thermal anomalies observed in these wells. This combination of enhanced permeability, deep circulation pathways, and favorable thermal conditions makes horst structures particularly conducive to the development of geothermal resources. As a result, the wells drilled into these horsts intersect zones of high thermal flow and fluid circulation, making them ideal sites for tapping into geothermal resources.

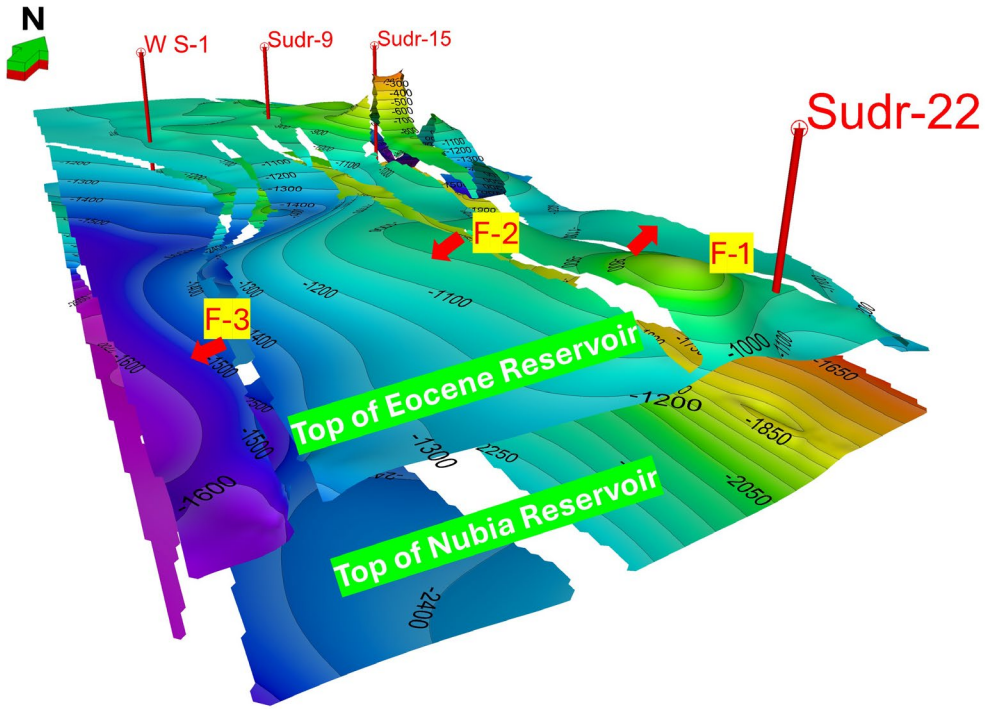

Figure 3: 3D structural model for Sudr oil field showing the interpreted tops, faults and horst structures controlling geothermal flow indie the field. The location of the three thermal wells is shown in addition to West Sudr-1 well (W S-1).

3.2. Resistivity Analysis

Analysis of resistivity logs (Fig. 4) reveals significant resistivity increases corresponding to Eocene geothermal reservoir zones, which consist of fractured limestone with resistivity values frequently exceeding 100 ohm·m. This characteristic high-resistivity signature is clearly evident in wells Sudr-9, Sudr-22, and W-S-1. The resistivity curves also demonstrate pronounced increases within evaporitic zones of the Miocene succession, while shale-rich Miocene intervals display correspondingly lower resistivity values due to their higher clay content and associated bound water. In contrast, the Nubian Sandstone reservoir (Sudr-15 well) does not exhibit the same elevated resistivity response as the Eocene carbonate geothermal reservoir. This discrepancy could be attributed to differences in lithology, porosity, or fluid salinity, as the Nubian Sandstone may host more saline water or have less effective fracture networks compared to the Eocene limestone. This could be evidenced by the high contrast in salinities of both reservoirs as indicated by drill stem tests of the studied wells, where the Eocene reservoir exhibits water salinity of about 9000 while the Nubian Sandstone shows salinities exceeding 200000 ppm.

Furthermore, specific intervals within the Miocene and Upper Cretaceous (particularly the Cenomanian) sediments also exhibit elevated resistivities, comparable to those of the Eocene reservoir. This aligns with hydrogeochemical studies (e.g., Issar et al., 1971; El-Kiki et al., 1992), which identify these intervals as potential water reservoirs within the Sudr oil field. Thus, resistivity signatures from well logs serve as a critical tool in identifying and characterizing geothermal reservoirs in a certain oil field.

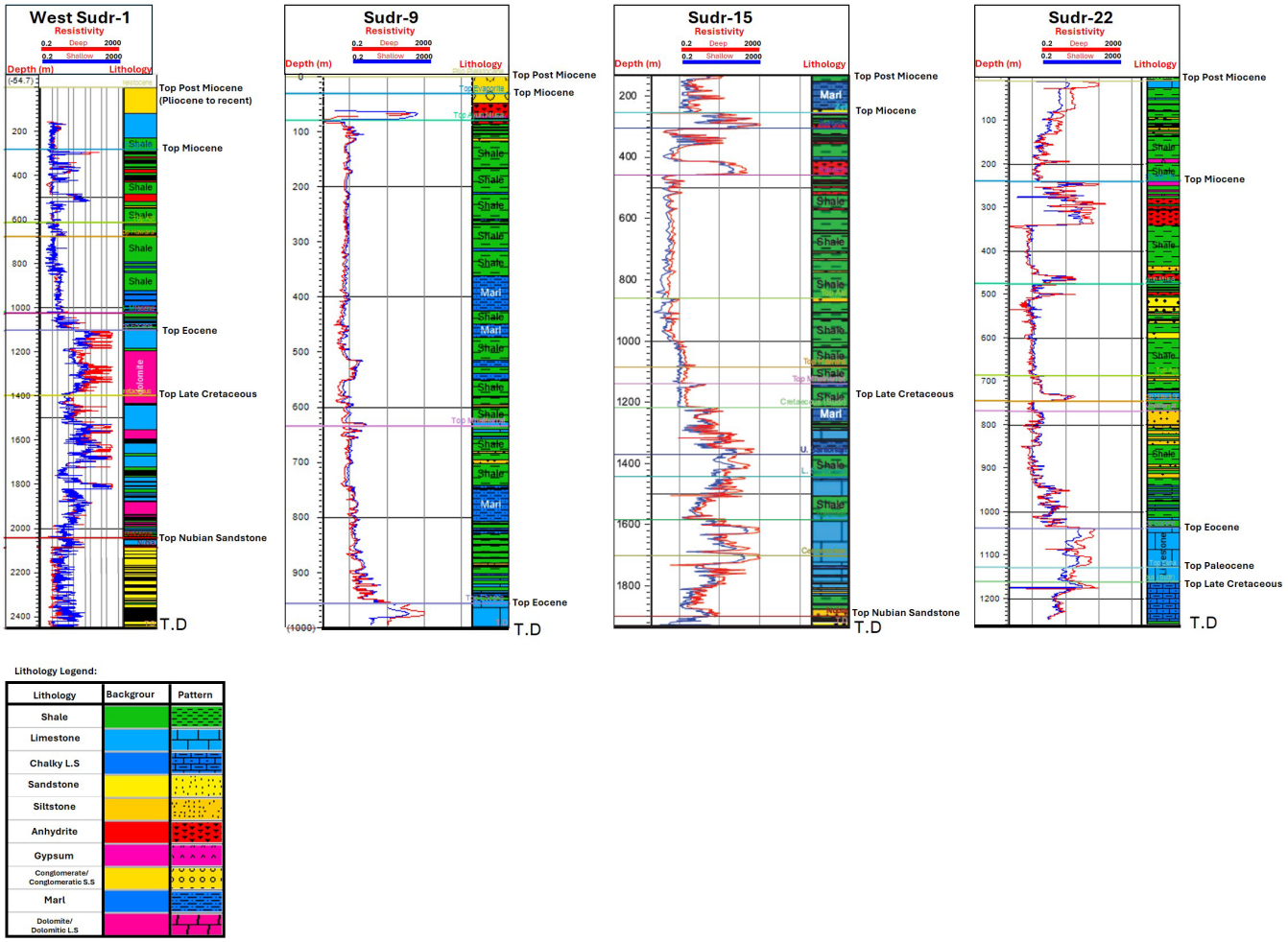

Figure 4: Geothermal resistivity analysis utilizing resistivity logs of four wells in Sudr field. A lithologic log is also displayed.

3.3. Temperature Assessment

Using the knowledge of 50 °C /km geothermal gradient and the measured surface temperature of the hot water at Sudr-22 well measured by the authors to be 86 °C, the estimated temperature at the top of the Eocene reservoir (at depth of 1 km) was calculated to be 76°C and the estimated temperature at the total depth of the well (1.25 km) is 88.5°C. When comparing the measured surface temperature of 86°C at the current well depth of 1.25 km with the theoretically expected temperature of 88.5°C at the same depth, a slight discrepancy of 2.5°C was observed. Temperature discrepancies observed in the assessment can be attributed to natural heat loss mechanisms such as conductive cooling and groundwater circulation, or alternatively to modeling uncertainties including surface temperature assumptions, geothermal gradient variations, and rock thermal conductivity heterogeneity (Sass et al., 1992; Beardsmore & Cull, 2001; Anderson, 2005; Clauser, 2006;). These minor discrepancies are generally considered within acceptable ranges for geothermal resource evaluations.

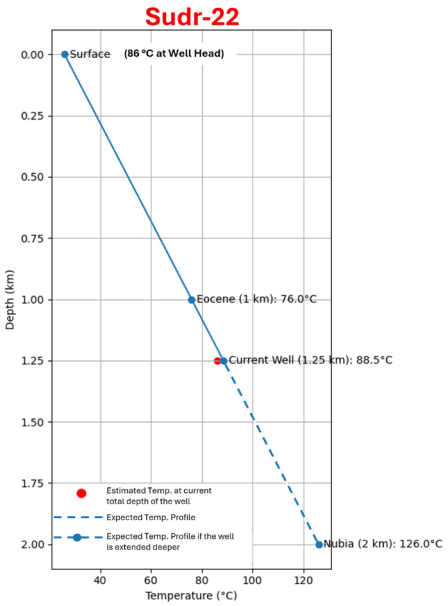

Figure 5: Temperature analysis for Sudr-22 well, showing expected temperature at different depths.

The projected temperature at the Nubia reservoir depth (2 km) reached 126°C. If Sudr-22 well were extended to reach the Nubia reservoir at 2 km depth, the estimated surface temperature at the wellhead would be approximately 123.5°C after accounting for the assumed temperature loss of 2.5°C during ascent. Fig. 5 shows the temperature analysis of Sudr-22 well.

3.4. Geothermal power potential

Based on the Monte Carlo simulation results (Fig. 6), the geothermal potential assessment of the Eocene reservoir reveals significant energy resources with considerable uncertainty ranges. The P50 (most likely) scenario indicates a recoverable thermal energy of approximately 6.34 PJ, translating to an average power generation capacity of 6.70 MW over the 30-year project lifetime. The P10 conservative estimate suggests a minimum recoverable energy of 2.90 PJ (3.06 MW), while the P90 optimistic scenario projects up to 12.04 PJ (12.73 MW). These estimates account for both rock matrix and pore fluid thermal contributions, with the rock matrix contributing approximately 76% of the total thermal energy due to its higher density and volume fraction compared to the pore fluids.

The wide uncertainty range between P10 and P90 values (a factor of ~4.2 difference in energy) reflects the inherent geological uncertainties in reservoir parameters, particularly reservoir extent, porosity distribution, and thermal gradient variations. The recovery factor distribution (8–20%, mode 12%) significantly influences the final estimates, emphasizing the importance of advanced geothermal extraction technologies for project viability. While the P50 power output approaches the 5-10 MW threshold for commercial geothermal development (e.g. Vimmerstedt 1998; Sanyal 2018), the P90 scenario suggests strong potential viability, particularly when considering the dual-purpose nature of the field for both hydrocarbon and geothermal energy extraction. These results indicate that detailed reservoir characterization and pilot testing would be essential to reduce uncertainties and optimize the geothermal development strategy for Sudr field.

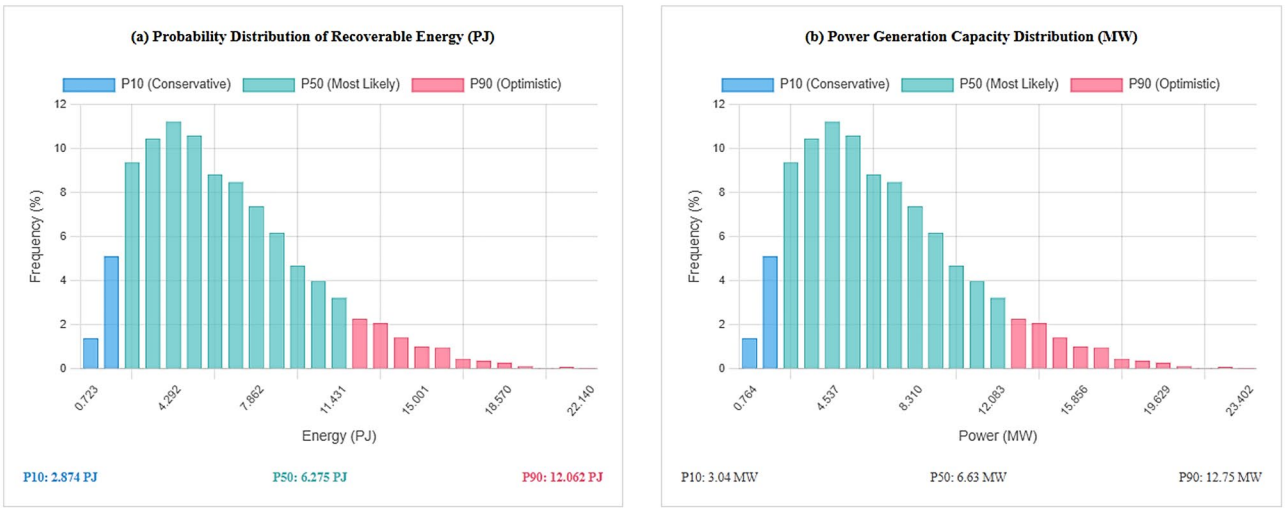

Statistical Summary and Key Findings

Parameter	P10 (Conservative)	P50 (Most Likely)	P90 (Optimistic)	Mean	Std Dev
Recoverable Energy (PJ)	2.874	6.275	12.062	6.963	3.641
Power Capacity (MW)	3.04	6.63	12.75	7.36	3.85

Figure 6: Monte Carlo simulation results for geothermal power potential assessment for Sudr oil field with statical summary and key findings listed.

CONCLUSIONS

The present pioneering geothermal study conducted at Sudr oil field in the Sinai Peninsula, Egypt concludes that:

- The field is structurally controlled by three Gulf of Suez rift-parallel faults that create horst structures, with one major rift-related fault bounding the Sudr field to the northeast.
- The normal faults and associated horst structures serve as geothermal heat concentrators and natural conduits, while controlling geothermal fluid flow within Sudr oil field.
- Reservoir temperatures of up to 126°C can be achieved at a geothermal drilling depth of 2 km.
- Resistivity log analysis revealed high resistivity values in the Eocene limestone geothermal reservoir and in the predicted Late Cretaceous reservoir, and very high resistivity for the evaporitic zones of the Miocene succession. However, resistivity is low in front of shaly zones of the Miocene and relatively lower in the Nubian Sandstone reservoir compared to the Eocene reservoir.
- Geothermal potential assessment of Sudr field indicates substantial energy resources, with a P50 recoverable thermal energy of approximately 6.3 PJ

(6.7 MW), a P10 estimate of approximately 2.9 PJ (3 MW), and a P90 projection of up to 12.1 PJ (12.8 MW) for a geothermal power plant with a 30-year operational lifetime supplying clean power to local households and tourist resorts.

ACKNOWLEDGEMENTS

We greatly acknowledge the Egyptian General Petroleum Corporation (EGPC) and Egyptian General Petroleum Company (GPC) for providing seismic and well log data that were fundamental to this study and for permission to publish this work. We extend our thanks to Prof. Shawky Sakran (Emeritus Professor of Structural Geology, Cairo University) for his insightful discussions that enhanced the manuscript, and to Mrs. Marwa Zayan from the Institute of Sustainable Processes, University of Valladolid, for her valuable assistance during this research.

REFERENCES

Anderson, M. P., 2005. Heat as a ground water tracer. Groundwater, 43(6), 951-968.

Aydin, H., Yüksel, S., & Topuz, C., 2024. Utilization of Oil and Gas Wells for Geothermal Applications. In Proceedings of the 49th Workshop on Geothermal Reservoir Engineering, Stanford University, Stanford, CA, USA (pp. 12-14).

Beardsmore, G.R., Cull, J.P., 2001. Crustal heat flow: a guide to measurement and modelling. Cambridge university press.

Boutot, J., Kang, M., 2025. Renewable energy production potential of abandoned and orphaned oil and gas wells and sites. Environmental Research Letters, 20(5), 054037.

Boulos, F.K., 1990. Some aspects of the geophysical regime of Egypt in relation to heat flow, groundwater and microearthquakes. In R. Said (Ed.), The geology of Egypt. A.A. Balkema, Rotterdam/Brookfield, pp. 61–89.

Clauser, C., 2006. Geothermal Energy, In: K. Heinloth (ed), Landolt-Börnstein, Group VIII: Advanced Materials and Technologies, Vol. 3: Energy Technologies, Subvol. C: Renewable Energies, Springer Verlag, Heidelberg-Berlin, 493-604.

EGPC, 1996. Gulf of Suez Oil Fields (A Comprehensive Overview); Egyptian General Petroleum Corporation, Cairo, Egypt, 736p.

El Ayouty, M.K., 1990. Petroleum geology, In R. Said (Ed.), The geology of Egypt. A.A. Balkema, Rotterdam/Brookfield, pp. 567–600.

EL Kiki, F.M., Eweida, E.A., EL Refeai, A.A., 1992. Hydrogeology of the Suez rift border province. Proceedings of the 3rd Conference Geology of Sinai for Development. Pp91–100 Ismailia, 1992.

Elzarka, M.H., 1975. Geochemical Relations of Fluids in Oil Fields of Gulf of Suez, Egypt: GEOLOGIC NOTES. AAPG Bulletin, 59 (9): 1667–1675.

Issar, A., Rosenthal, E., Eckstein, Y., Bogoch, R., 1971. Formation waters, hot springs and mineralization phenomena along the eastern shore of the Gulf of Suez. International Association of Scientific Hydrology. Bulletin 16, 25–44.

Jolie, E., Faulds, J. and Moeck, I., 2012. The development of a 3D structural–geological model as part of the geothermal exploration strategy—a case study from the Brady's geothermal system, Nevada, USA. In Proceedings, thirty-seventh workshop on geothermal reservoir engineering, Stanford University (pp. 421-5).

Meenakshisundaram, A., Tomomewo, O. S., Aimen, L., Bade, S. O., 2024. A comprehensive analysis of repurposing abandoned oil wells for different energy uses: Exploration, applications, and repurposing challenges. Cleaner Engineering and Technology, 22, 100797.

Moeck, I.S., 2014. Catalog of geothermal play types based on geologic controls. Renewable and sustainable energy reviews, 37, pp.867-882.

Moustafa, A.R., 2004. Geological maps of the eastern side of the Suez Rift (Western Sinai Peninsula), Egypt. AAPG/Datapages. American Association of Petroleum Geologists.

Poux, B. and Banks, G., 2022. Visualize and Communicate Confidence in 3-D Geological Models for Geothermal Exploration and Development. In Proceedings of the Geothermal Rising Conference (GRC).

Poux, B. and O'Brien, J., 2020. A Conceptual Approach to 3-D Play Fairway Analysis for Geothermal Exploration and Development. In Proceedings 42nd New Zealand Geothermal Workshop (Vol. 24, p. 26). NZ Geothermal Association.

Santos, L., Taleghani, A. D., Elsworth, D., 2022. Repurposing abandoned wells for geothermal energy: Current status and future prospects. Renewable Energy, 194, 1288-1302.

Sanyal, S.K., 2018. Geothermal Power Economics. In: Bronicki, L. (eds) Power Stations Using Locally Available Energy Sources. Encyclopedia of Sustainability Science and Technology Series. Springer, New York, NY.

Sass, J. H., Lachenbruch, A. H., Moses Jr, T. H., Morgan, P., 1992. Heat flow from a scientific research well at Cajon Pass, California. Journal of Geophysical Research: Solid Earth, 97(B4), 5017-5030.

Zarrouk, S. J., Moon, H. (2014). Efficiency of geothermal power plants: A worldwide review. *Geothermics*, *51*, 142-153.